SUPPLEMENTAL INFORMATION

Stromal-initiated changes in the bone promote metastatic niche development

Xianmin Luo†, Yujie Fu†, Andrew J. Loza, Bhavna Murali, Kathleen M. Leahy, Megan K. Ruhland, Margery Gang, Xinming Su, Ali Zamani, Yu Shi, Kory J. Lavine, David M. Ornitz, Katherine N. Weilbaecher, Fanxin Long, Deborah V. Novack, Roberta Faccio, Gregory D. Longmore, Sheila A. Stewart

†These authors contributed equally to the work.

Luo & Fu et al., Supplementary Figure S1

A

	OCN+	
4 mice	GFP-%	GFP+%
1-1	39.78	60.22
1-2	22.42	77.58
1-3	55.05	44.95
1-4	36.96	63.04
1-5	25.00	75.00
2-1	47.95	52.05
2-2	36.69	63.31
2-3	42.00	58.00
2-4	51.43	48.57
2-5	57.34	42.66
3-1	73.97	26.03
3-2	73.86	26.14
3-3	59.34	40.66
3-4	49.12	50.88
3-5	57.26	42.74
4-1	95.12	4.88
4-2	78.08	21.92
4-3	76.77	23.23
4-4	84.03	15.97
4-5	83.11	16.89

B

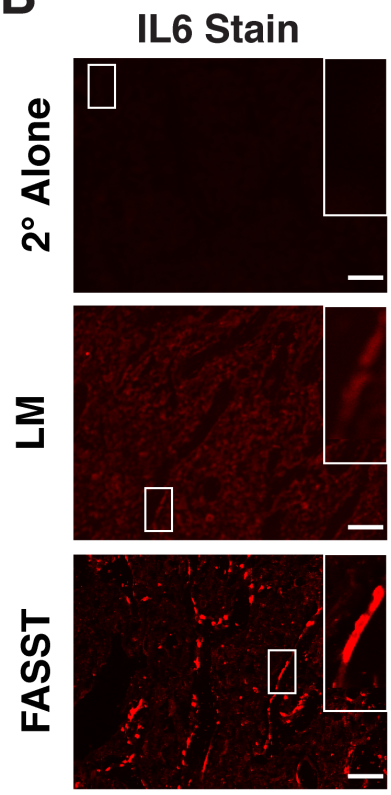

C

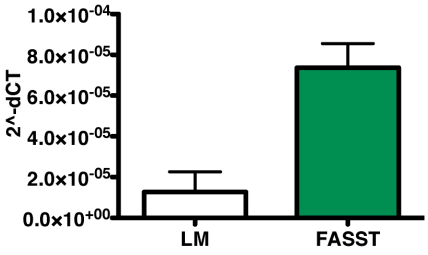

D

E

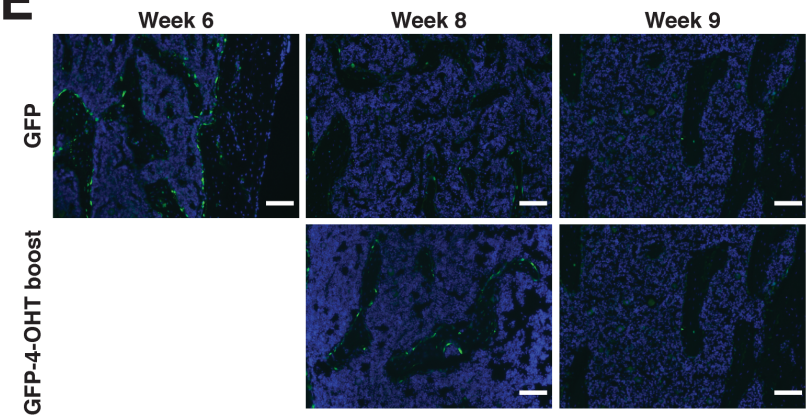

F

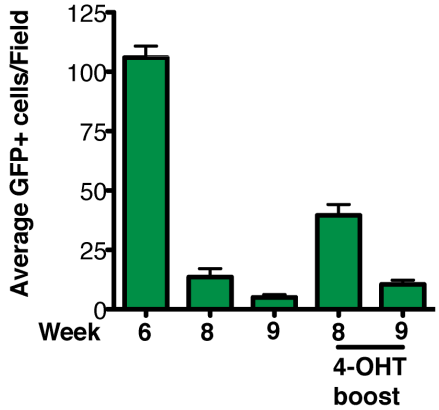

Figure S1, related to Figure 1. Quantification of transgene activation and senescent osteoblasts in FASST mice reveal varied penetrance of GFP activation.

(A) Mice received IP injections of 4-OHT at week 4 and transgene activation was monitored at week 6 by staining bone sections from FASST mice with antibodies against GFP and osteocalcin (OCN). GFP activation was quantitated in 5 sections from 4 different mice. The table displays the percent of OCN-positive cells that were negative or positive for GFP expression. (B) Secondary antibody panel and corresponding LM and FASST IL6 stains (also shown in **Figure 1D**) is shown for comparison. Scale bar 100 um. (C) FASST mice express more IL-6 mRNA than littermate (LM) control mice. Mice received 4-OHT at 4 weeks and mRNA was made from tail vertebrate at 6 weeks. (D) Timeline of 4-OHT treatment. Mice received IP injections of 4-OHT at week 4 and transgene activation was monitored at weeks 6, 8 and 9. A second group of mice received a 4-OHT boost at 6 weeks and GFP activation was monitored at weeks 8 and 9 (2 and 3 weeks after the boost that occurred at 6 weeks). (E) Bone sections from FASST mice were stained with anti-GFP (green) to identify transgene activation and nuclei were counterstained with DAPI. Representative images show that transgene activation was observed exclusively in the trabecular regions. Scale bar 100 μm. (n= 3 mice). (F) Quantification of transgene activation depicted in E (n=3 mice).

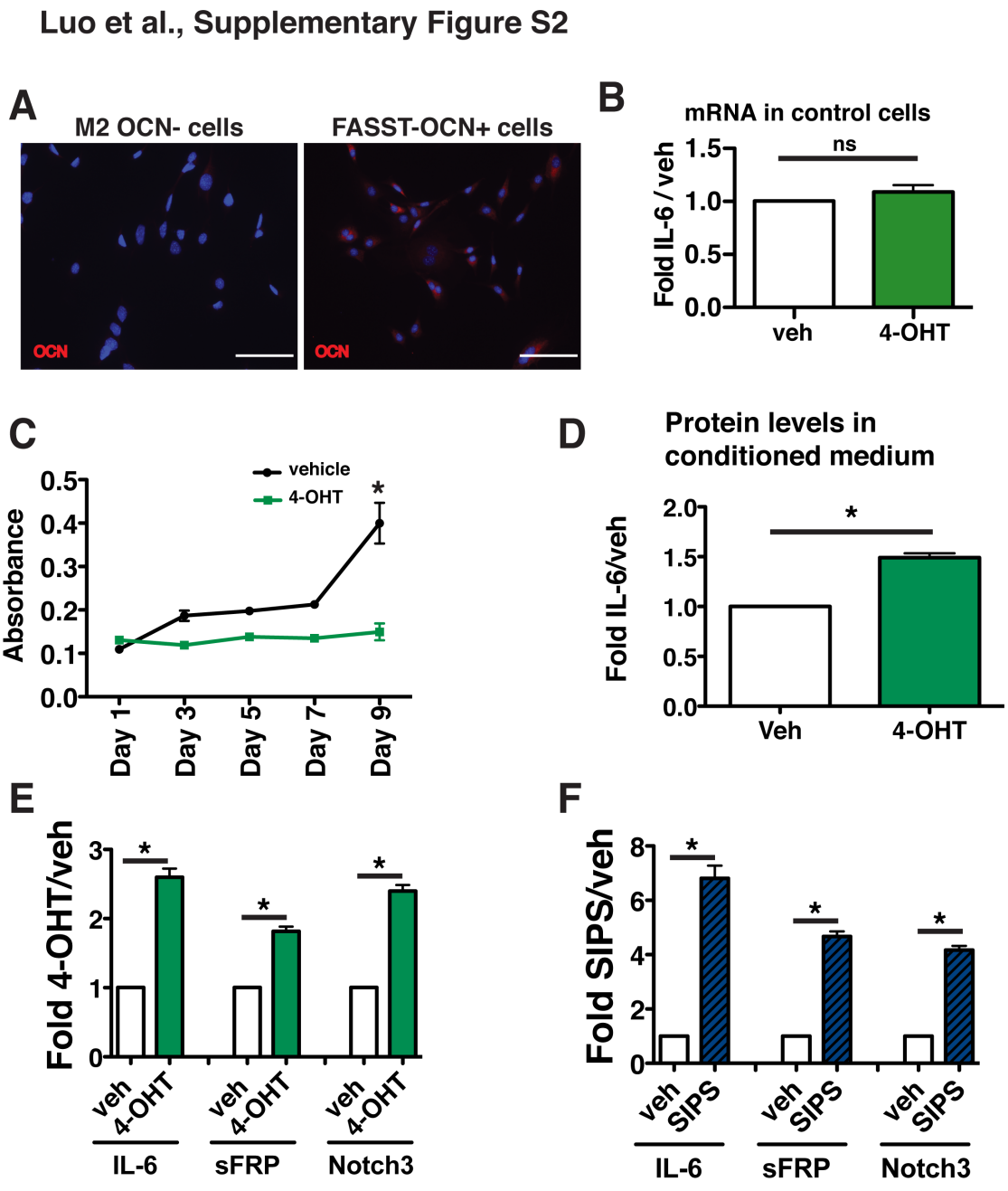

Figure S2 related to Figure 3. FASST osteoblasts senesce after 4-OHT treatment *in vitro*.

(A) Osteoblasts were isolated from FASST mice (right panel) and stained with an anti-OCN antibody. M2 bone stromal cells do not express OCN and serve as a negative antibody control (left panel). Nuclei were counterstained with DAPI.

Scale bar 200 μm. (B) Vehicle and 4-OHT treatment of osteoblasts that do not express Cre-ER^{T2} demonstrate that 4-OHT does not induce IL-6 expression (n=2, NS, not significant). (C) MTT growth assay on vehicle (veh) or tamoxifen (4-OHT) treated osteoblasts from FASST mice treated *ex vivo* demonstrate that 4-OHT treatment leads to a robust growth arrest (*p<0.05, two-way ANOVA). (D) IL-6 protein levels present in FASST osteoblasts cultures treated with vehicle or 4-OHT (n=2, SEM, *p<0.05). (E) SASP expression in osteoblasts following p27^{Kip} expression. qRT-PCR expression of IL-6, sFRP, and Notch 3 in vehicle (veh) versus 4-OHT treated osteoblasts grown in osteogenic medium. (SEM, *p<0.05, two-tailed, Student t test). (F) SASP expression in osteoblasts following bleomycin treatment. qRT-PCR expression of IL-6, sFRP, and Notch3 in vehicle (veh) versus bleomycin (stress-induced premature senescence, SASP) treated osteoblasts grown in osteogenic medium. (SEM, *p<0.05, two-tailed, Student t test).

Luo & Fu et al., Supplementary Figure S3

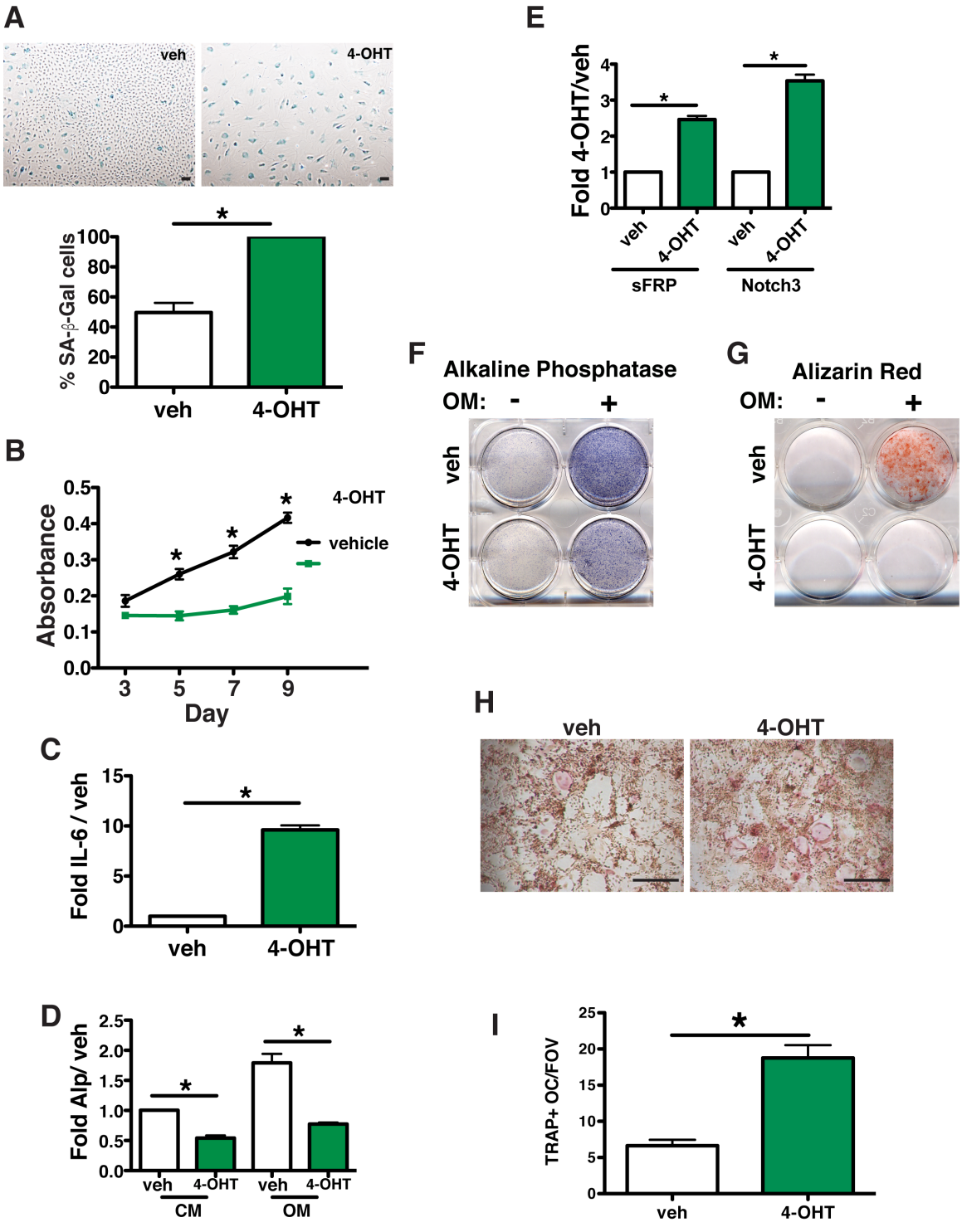

Figure S3, related to Figure 3. Senescence induced by loss of the telomere binding protein, TRF2, alters osteoblast gene expression and induces SASP

(A) Primary osteoblasts were obtained from the femurs of 6-week-old FASST-TRF2 mice. To delete TRF2 from osteoblasts and induce senescence, FASST-TRF2 osteoblasts were treated with 10μM tamoxifen (4-OHT) for 3 days *ex vivo*. SA-β-Gal staining was carried out on 4-OHT or vehicle (veh) treated osteoblasts on day 3. 4-OHT treatment resulted in a significant increase in SA-β-Gal positive cells compared to vehicle treated cells (SEM, *p<0.05, two-tailed, Student t test). Scale bar 100 um. (B) MTT growth assay on vehicle of tamoxifen (4-OHT) treated osteoblasts from FASST-TRF2 mice treated *ex vivo* demonstrate that 4-OHT treatment leads to a robust growth arrest (SEM, *p<0.05, two-way ANOVA). (C) The induction of the senescence-associated secretory phenotype (SASP) factor IL-6 was evaluated by quantitative reverse transcriptase PCR (qRT-PCR). Senescent osteoblasts from FASST-TRF2 mice expressed significantly more *IL-6* mRNA compared to vehicle (veh) treated cells (SEM, *p<0.05, two-tailed, Student t test). (D) qRT-PCR expression of alkaline phosphatase (*ALP*) in vehicle (veh) versus 4-OHT treated osteoblasts grown in basic culture medium (CM) versus osteogenic culture medium (OM). Senescent osteoblasts from FASST-TRF2 mice displayed a dramatic reduction in *ALP* mRNA levels. (SEM, *p<0.05, two-tailed, Student t test). (E) SASP expression in osteoblasts following TRF2 deletion. qRT-PCR expression of sFRP and Notch 3 in vehicle (veh) versus 4-OHT treated osteoblasts grown in osteogenic medium. (SEM,

*p<0.05, two-tailed, Student t test). (F) ALP staining in senescent (4-OHT) versus non-senescent (veh) osteoblasts. FASST-TRF2 osteoblasts were treated with vehicle or 4-OHT *ex vivo* for 3 days and then plated in basic culture medium (-) versus osteogenic culture medium (+) for 3 days. ALP expression was assessed on day 7. 4-OHT treated osteoblasts displayed a robust reduction in ALP expression. (G) Alizarin Red-S staining in senescent (4-OHT) versus non-senescent (veh) osteoblasts. FASST-TRF2 osteoblasts were treated with vehicle or 4-OHT *ex vivo* for 3 days and then plated in basic culture medium (-) or osteogenic medium (+) for 3 days. Mineralization capacity was assessed by staining with Alizarin Red-S on day 21. 4-OHT treated osteoblasts displayed a robust reduction of mineralization capability. (H) Senescent osteoblasts increase osteoclastogenesis. Representative images of FASST-TRF2 osteoblasts treated with vehicle (Veh) or 4-OHT *ex vivo* for 3 days. 4-OHT was than removed from the culture medium and on day 12, after robust activation of senescence (data not shown) bone marrow macrophages from wildtype mice were plated on non-senescent versus senescent osteoblasts and osteoclastogenesis was determined by TRAP staining on day 16. Scale bar 200 μm. (I) Quantification of TRAP-positive osteoclasts (TRAP+OC) in the presence of nonsenescent (veh) or senescence (4-OHT) osteoblasts from panel C. Data are presented as TRAP+OC/field of view (TRA+OC/FOV). (*p<0.05, two-tailed, Student t test).

Luo & Fu et al., Supplementary Figure S4

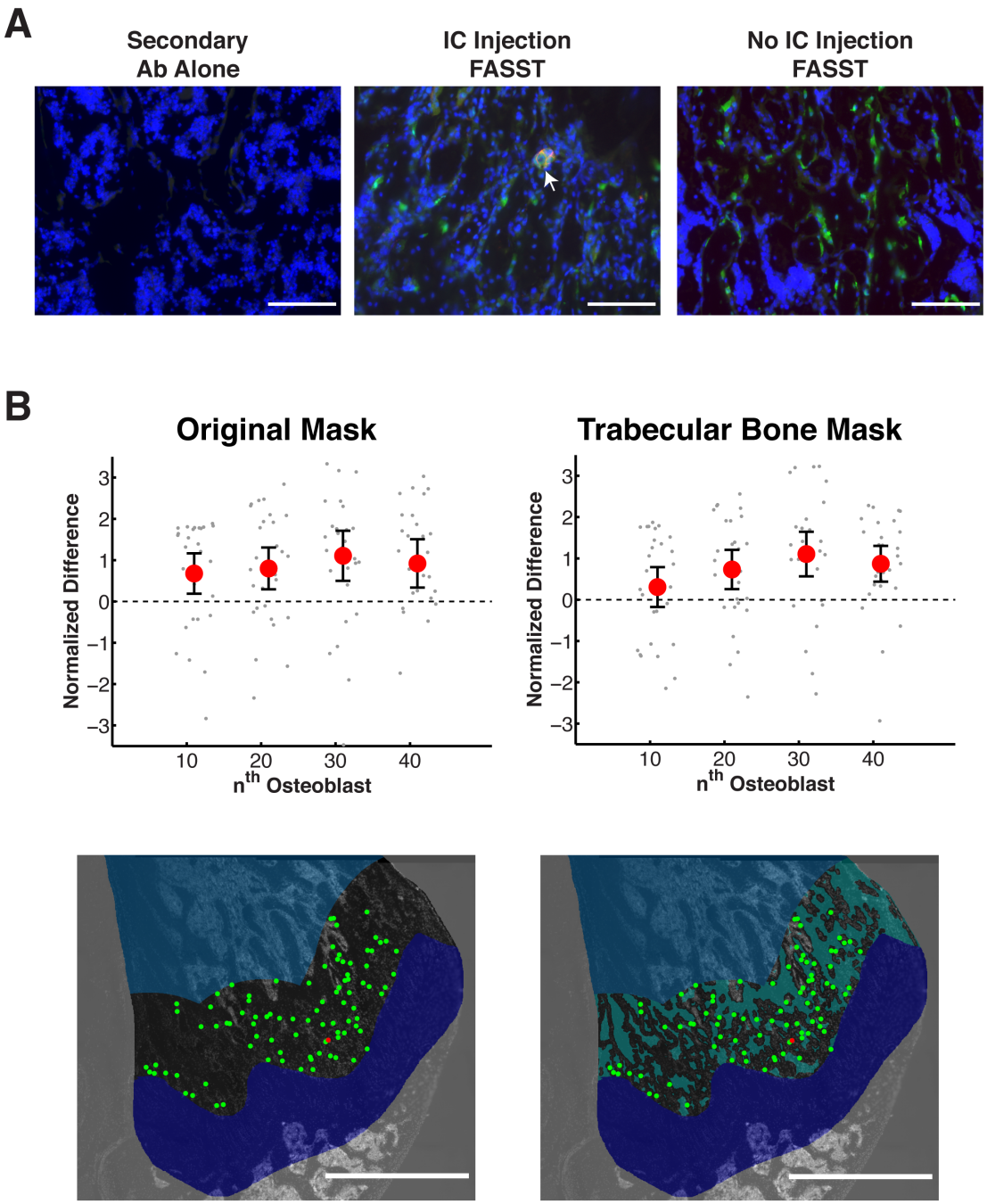

Figure S4 related to Figure 5. Controls for tumor cell seeding analyses

(A) FASST bones were stained after intracardiac injection of tumor cells with a secondary antibody alone (left) or an anti-EpCAM and secondary antibody (middle,

arrow points to tumor cell cluster). Bones from a FASST mouse that was not injected with tumor cells (right) was also stained with an EpCAM and secondary antibody as described for Figure 5. Scale bar 100 um. Note: tumor cells express GFP. (B) Computational spatial analysis of tumor cell localization as originally shown in Figure 5 (left) is presented against a control experiment (right) in which the trabecular bone regions were masked out of the analyses and placement of osteoblasts was restricted to a thin region (30um thick) along the surfaces of trabecular bone. Thus, this analysis only examined areas where osteoblasts should be found. Scale bar 1 mm.

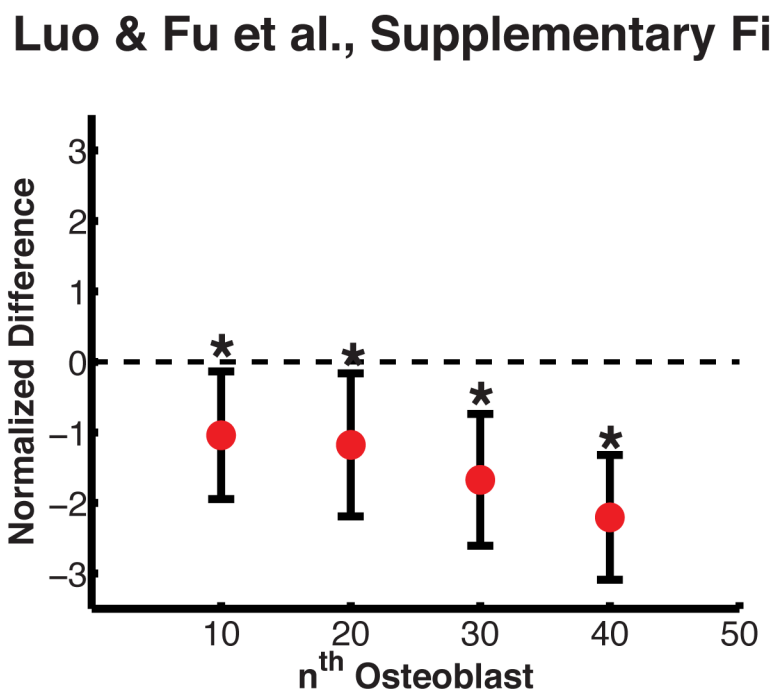

Figure S5 related to Figure 5. Tumor cells localize to senescent osteoblasts

The likelihood that a tumor cell would encounter a senescent osteoblast by chance (dotted line at 0) versus the observed frequency was calculated for each osteoblast. Osteoblast locations were sampled instead of tumor cell locations to minimize edge

effects associated with tumor cells located near the border of the region of interest. Following the sampling, the mean, standard deviation, median, and 95% confidence interval were computed. To better visualize the difference between the observed and expected distance distributions, the ratio of the observed and expected median distance functions was taken. Where this plot is greater than 1, the distance to the n^{th} senescent osteoblast from a tumor cell was larger than expected, favoring segregation of the two cell populations. Where this plot is less than 1, the distance from a tumor cell to the n^{th} nearest senescent osteoblast is smaller than expected, thus favoring association of the two populations. To allow for combination of data across multiple samples and mice, a normalized difference (also referred to as effect size) curve was computed. The difference between the observed distance and mean difference for the n^{th} nearest osteoblast was taken and normalized by sampling standard deviation. The resulting curve provides a measure of how many standard deviations away from the random mean the observed results lie (*p values for the 10^{th}, 20^{th} , 30^{th} , and 40^{th} osteoblasts is 0.039, 0.037, 0.003, and 0.0002, respectively). Data are from one femur bone and is a representative of the three bones analyzed.

Luo & Fu et al., Supplementary Figure S6

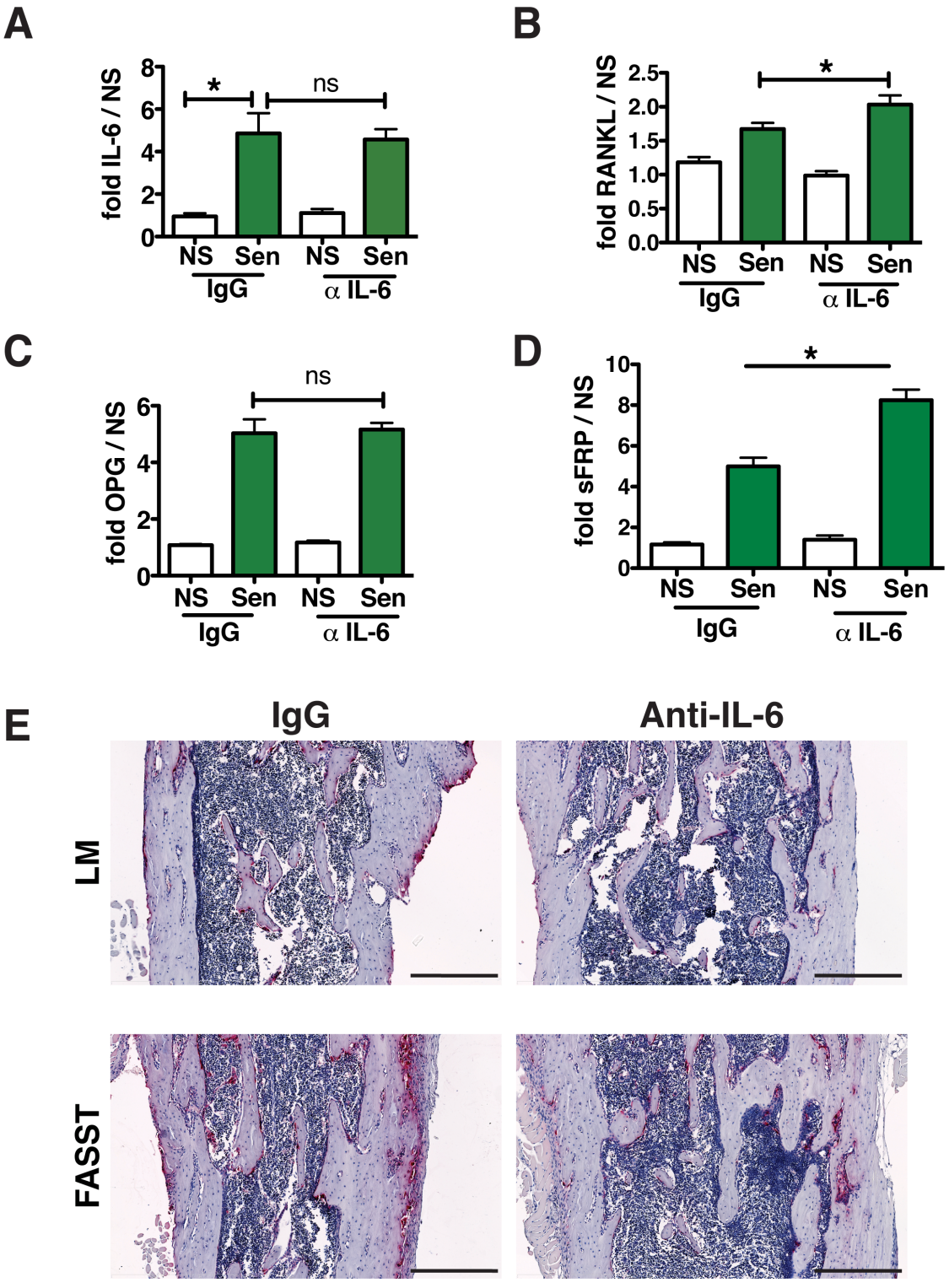

Figure S6 related to Figure 6. Neutralization of senescent osteoblast derived IL-6 fails to impact the induction of senescence

(A) Non-senescent (NS) or senescent (Sen) FASST osteoblasts were treated *ex vivo* with a control IgG or anti-IL-6 (α IL-6) for 4 days. On day 4, total mRNA was extracted qRT-PCR was carried out for IL-6 and no differences were observed in IL-6 expression in senescent osteoblasts treated with IgG or anti-IL-6, indicating that anti-IL-6 had no impact on SASP expression in senescent osteoblasts (*$p<0.05$, two-tailed, Student t test). (B) Non-senescent (NS) or senescent (Sen) osteoblasts were treated *ex vivo* with a control IgG or anti-IL-6 (α IL-6) for 4 days. On day 4, total mRNA was extracted qRT-PCR was carried out for RANKL. No differences were observed in senescent FASST osteoblasts treated with IgG compared to anti-IL-6 (*$p<0.05$, two-tailed, Student t test). (C) Non-senescent (NS) or senescent (Sen) FASST osteoblasts were treated *ex vivo* with a control IgG or anti-IL-6 (α IL-6) for 4 days. On day 4, total mRNA was extracted and qRT-PCR was carried out for OPG. No differences were observed in senescent FASST osteoblasts treated with IgG compared to anti-IL-6 (*$p<0.05$, two-tailed, Student t test). (D) Non-senescent (NS) or senescent (Sen) FASST osteoblasts were treated *ex vivo* with a control IgG or anti-IL-6 (α IL-6) for 4 days. On day 4, total mRNA was extracted and qRT-PCR was carried out for sFRP1. A small increase in sFRP1 was observed in senescent FASST osteoblasts treated with IgG compared to anti-IL-6 (*$p<0.05$, two-tailed, Student t test). (E) Representative bone sections from 6-week-old FASST or littermate (LM) control mice treated with an IgG control or anti-IL-6 antibody were used to assess osteoclast surface

to bone surface area by TRAP staining where osteoclasts are indicated by red, TRAP+ staining and nuclei are counterstained with hematoxylin. Scale bar 100 μm (n=3).

SUPPLEMENTAL EXPERIMENTAL PROCEDURES

Mice husbandry and genotyping. All mice were housed in accordance with Washington University in St Louis's Animals Studies Committee. To obtain stromal specific activation of a lox-stop-lox cassette mice expressing a chimeric gene encoding the Cre-ER^{T2} fusion protein, which allows for tamoxifen-dependent recombination under the control of a mesenchymal-specific regulatory sequence derived from the pro-alpha 2(I)collagen gene (Col-Cre-ER^{T2} mice, kind gift of Benoit de Crombrugghe, M.D. Anderson Cancer Center, Houston, Texas, USA, and Christopher Denton, Center for Rheumatology, Royal Free and University College Medical School, London, United Kingdom) (Zheng et al., 2002) were intercrossed with mice that conditionally express the cell cycle inhibitor, *p27 ^{Kip1}* from the ROSA26 locus (ROSAlox-stop-lox-*p27^{Kip1}*) (Lavine et al., 2008). Cre-ER^{T2} was maintained in the hemizygous state and the conditional *p27 ^{Kip1}* allele was maintained in the homozygous state. Finally, mice were subject to speed congenics and bred to a pure FVB background.

Mouse genotyping was carried out as follows: genomic DNA was extracted from mouse tissue using the RED Extract N Amp kit (XNAT, Sigma, St. Louis, MO). Primer sequences used to determine the presence of the *p27^{Kip1}* transgene within

the ROSA26 locus were as follows: the wildtype ROSA26 locus was amplified using 3' wt: GGA GCG GGA GAA ATG GAT ATG AAG TAC TGG (forward) and 5': CAA AGT CGC TCT GAG TTG TTA TCA GTA AGG (reverse) and the *p27 ^{Kip1}* containing locus was amplified using 3' wt: GGA GCG GGA GAA ATG GAT ATG AAG TAC TGG (forward) and 3'delta: TCC AAG AGT ACT GGA AAG ACC GCG AAG AGT (reverse). Primer sequences used to amplify the Cre-ER^{T2} transgene were 3': ATC CAG GTT ACG GAT ATA GT (forward) and 5': ATC CGA AAA GAA AAC GTT GA (reverse).

To amplify DNA of interest, 1µl DNA extract was combined with 9µl of master mix (XNAT kit with 0.5uM appropriate forward and reverse primers) in PCR tubes and amplified for one cycle at 94°C for 1 minute followed by 35 cycles at (94°C for 30 seconds, 58°C for 60 seconds, and 72°C for 60 seconds) and a 4°C hold. PCR products were resolved on a 1% agarose/TAE (BP160, Fisher Scientific, Pittsburgh, PA) containing 0.002% SyberSafe (UV gel stain, S33102, Invitrogen, Carlsbad, CA) gel at 100 volts for 45 minutes, and visualized with UV light.

Transgene activation and Intracardiac Injection (IC). Four-week-old FASST female mice and control littermates were given tamoxifen (5mg/10g body weight) intraperitoneal (IP) administration twice. Since the half-life of osteoblasts is about fourteen days (Park et al., 2012), we boosted mice with an additional dose of tamoxifen at six weeks of age to increase the percent of senescent osteoblasts within the bones of young mice. Analysis of these mice revealed that the additional

tamoxifen increased the presence of GFP-positive osteoblasts relative to mice that did not receive the tamoxifen boost (**Figure S2**). On the day of IC injection, mice were anesthetized with 100μL/ 20g body weight of Ketamine/xylazine cocktail (17.7mg/ml of ketamine and 2.65mg/ml1 of xylazine). When animals were completely anesthetized, 50 μL of NT2.5 cells expressing firefly luciferase (10,000 cells/50ul PBS) were injected directly into the left cardiac ventricle. Bioluminescence imaging was performed on day 3, 7, 14, 21 and 30 post-IC injection on an IVIS100 or IVIS Lumina (PerkinElmer, Downers Grove, IL; Living Image 3.2, 1-60sec exposures, binning 4, 8 or, 16, FOV 15cm, f/stop1, open filter) following IP injection of D-luciferin (150mg/kg; Biosynth, Naperville, IL). For analysis, total photon flux (photons/sec) was measured from a fixed region of interest over the xenografts using Living Image 2.6. At week 4, bones were imaged *ex vivo*. Animals were sacrificed immediately following day 30 imaging and both femoral and tibia bones were isolated and imaged. To control for any unanticipated effects of tamoxifen in the system, both FASST and littermate control mice received tamoxifen.

Bone histomorphology and tartrate-resistant acidic phosphatase (TRAP) staining. Mouse femur or tibia bones were isolated and fixed in 10% neutral buffered formalin for 24 hours. Bones were decalcified in 14% EDTA for 14 days at 4^{o}C embedded in paraffin and sectioned at the histology core of the Washington University Musculoskeletal Research Center. Standard H&E technique was used for all bone sections. The TRAP staining was performed as previously described

(Tsuboi et al., 2003). Images were collected using the NanoZoomer slide scanner, Alafi Neuroimaging Laboratory. To quantitate the TRAP positive cells and determine how much of their surface area covered the bone (i.e. OcS/BS) we used the BioQuant software to quantitate osteoclasts in the tibia near the growth plate. We carried out these measurements by defining a region of interest with the stamp tool window. We then chose a diagonal line type and set the distance to growth plate and measured the OcS/BS.

Fluorescence-based TRAP was performed using ELF97 phosphatase substrate Kit (Molecular Probes, E6601; Invitrogen) (Filgueira, 2004) followed by staining with antibodies against GFP and OCN. Slides were washed thoroughly in PBS, immersed in ELF97 phosphatase substrate buffer for 2 minutes and the reaction was stopped by submerging slides in wash buffer (PBS, 25mMEDTA, 5mM levamisol, pH 8.0) for 30 minutes, mounted in ELF 97 mounting medium, and visualized.

Senescent-associated ß-galactosidase (SA-ß-Gal) and immunofluorescence/ immunocytochemistry staining (IF/IHC). All SA-ß-Gal and immunofluorescence staining were carried out on cryosections. To prepare cryosections, mouse femur or tibia bones were isolated and fixed in 4% paraformaldehyde in PBS for 24 hours at 4ºC. Bones were decalcified in 14% EDTA for 2 days at 4ºC, immersed in 30% sucrose overnight, then were embedded in OCT and sectioned and stored at -80ºC. 8 µM cryosections were used for SA-ß-Gal staining. Immunofluorescence staining:

slides were permeabilized in 0.5% Triton X-100/PBS for 10 minutes at room temperature (RT) and blocked in DAKO protein block solution (Dako, X0909, Carpinteria, CA) for 30mins at RT. Slides were incubated following primary antibody stain in antibody diluent solution (Dako, S3022, Carpinteria, CA) overnight at 4ºC. Anti-GFP (1:1000, ab13970; Abcam, Cambridge, MA), anti- IL-6 (M-19, (1:50, SC-1265; Santa Cruz Biotechnology, Santa Cruz, CA), and anti-Osteocalcin (1:50, SC-30045; Cruz Biotechnology, Santa Cruz, CA) were used to stain sections. Following incubation with primary antibodies the slides were washed in PBS and incubated for 1 hr with appropriate Alexa fluor secondary antibodies at RT. After immunolabeling, the sections were washed in PBS and mounted in ProLong Gold with DAPI antifade medium. The sections were examined using a Nikon fluorescence microscope.

Luciferase labeling of NT2.5 cells and culture conditions. Mouse mammary tumor cell line NT2.5 was kindly provided by Dr. Jaffee from John Hopkins University School of Medicine. Baltimore were maintained in RPMI supplemented with 20% fetal bovine serum (FBS), 1.2% HEPES, 1% L-glutamine, 1% non-essential amino acids, 1% sodium pyruvate, 0.2% gentamycin, and 0.2% insulin. The FUW-firefly luciferase-enhanced green fluorescent protein (FUW-FFLuc-eGFP) lentiviral construct was obtained from Dr. David Piwnica-Worms (MD Anderson, Houston, TX). The lentivirus production and infection were carried by first transfecting 293T cells with FUW-FFLuc eGFP DNA, pCMVΔR8.2 and pCMV-VSV-G (8:1 ratio) using TransIT-LT1(Mirus, Madison, WI). Virus was collected 48 h

post-transfection, NT2.5 cells were infected and GFP+, productively infected cells were isolated by FACS. To measure luciferase activity, NT2.5 FFluc eGFP cells (NT2.5luc) were plated into 96 well, D-Luciferin was added to each well and plates were imaged using bioluminescence IVIS 100.

To establish the impact of conditioned medium on NT2.5luc cell growth, conditioned medium was collected from senescent or nonsenescent FASST osteoblasts and NT2.5luc cell growth was monitored by luciferase activity. For IL-6 neutralization experiments, NT2.5 cells were cultured in the conditioned medium from either senescent or nonsenescent osteoblasts plus 10pg/µl IL-6 neutralization antibody (Cat#554400, BD Biosciences, San Jose, CA 95131) or IgG control (Cat#40041B, BioLegend, San Diego, CA 92121). On day 3, NT2.5 cell growth was assessed by monitoring luciferase activity.

IL-6 neutralization in mice. One day prior to tamoxifen injection FASST or littermate control mice received either rat anti-murine IL-6 antibody (500 µg/mouse, BioXCell, West Lebanon, NH) or rat anti-murine IgG2a control antibody (500 µg/mouse, BioXCell, West Lebanon, NH) via intraperitoneal (IP) injection. Mice continued to receive additional antibody twice a week until sacrifice.

Image Acquisition. Images were acquired using a Nikon Eclipse Ti-E microscope with automated stage and focus control driven by Metamorph Software. To acquire images over a large spatial range when required, slides were scanned, and the

resulting sets of individual images were assembled into a single large image after correcting for illumination artifacts using a custom Matlab (MathWorks; Natick, MA) program.

Osteoclast-Osteoblast Spatial Analysis

Cell Identification: Cell identification was performed using custom Matlab software. A preliminary binary image showing regions corresponding senescent osteoblasts was computed by intensity and size thresholding of fluorescence images of endogenous GFP. Preliminary non-senescent osteoblasts were identified in the same manner using osteocalcin immunofluorescence images. The intersection of these two preliminary binary images was used as the final senescent osteoblast binary image. The final non-senescent osteoblast binary image was computed by subtracting the final senescent binary image from the preliminary non-senescent binary image. Due to the closely spaced nature of osteoblasts, rather than segmenting individual cells, these final binary images were used to mask the respective original images such that signal was kept only in regions identified as osteoblasts of the appropriate type. Osteoclasts were identified using intensity thresholding and morphological closing to create a binary image.

Spatial Analysis: The distribution of observed senescent or non-senescent osteoblasts fluorescent signal relative to osteoclasts was computed by determining the fraction of total true osteoblast signal within each distance bin. This was normalized by the expected amount of osteoblast signal in the case of uniform

distribution relative to osteoclast location. The relative likelihood calculation is formally summarized in the following equation:

$$S(d) = \frac{\sum D_{ij}(d) M_{ij} I_{ij}}{\sum D_{ij}(d)\, I^*_{ij}}, \qquad (1)$$

Where d specifies the distance bin, summation is performed over all rows (i) and columns (j) in the image, D_{ij} is a distance indicator matrix taking a value of 1 if D_{ij} matches the distance bin d and 0 otherwise, M_{ij} is the osteoblast indicator matrix taking a value of 1 if M_{ij} was identified as a positive osteoblast pixel in the masking step, I_{ij} is the true intensity image, and I^*_{ij} is the uniformly distributed intensity image. Therefore, if $S(d)$ takes a value greater than 1, more osteoblast fluorescence intensity was observed in that region than would be expected if intensity were uniformly randomly distributed in the image.

Senescent Osteoblast-Tumor Cell Analysis

Cell Identification: Tumor cells within the bone were defined as contiguous clusters of 1 or more individual cells staining positive for EpCAM. The location of each cell or contiguous cluster was manually determined using ImageJ. A custom Matlab program was used to automatically identify senescent osteoblasts guided by user input. Due to variability in staining intensity and background between slices, a manually determined intensity cutoff was used to threshold GFP channel images. These thresholded images were cleaned using one round of morphological opening

and then subject to a size threshold. The centroids of remaining objects were recorded as locations of senescent osteoblasts.

Region of Interest Identification: The regions in space where tumor cells and osteoblasts may be found do not necessarily correspond directly to the entire regions imaged. For senescent osteoblast-tumor cell localization, the region of interest was defined as within the bone and extending from the growth plate to a distance of 500μm away from the growth plate down the diaphysis. This region was selected because tumor cells were never observed within the growth plate and were not observed farther than 500μm away from the growth plate. To control for the presence of solid bone within this region and possible spatial bias due to its presence, supplemental analyses restricted osteoblast identification and subsequent placement in random sampling to only the surfaces of trabecular bone (**Figure S6B**). Trabecular bone was identified by thresholding the GFP channel tiled images to identify areas with low fluorescence signal (solid bone) within the original region of interest. The borders of these regions were identified and the new region of interest used in osteoblast detection and placement was defined as a 30um thick band centered on this border.

Spatial Analysis: To determine if the location of tumor cells within the bone was associated with the location of senescent osteoblasts, we employed techniques of spatial point process analysis similar to those developed by Perry and Ripley(Perry, 1995{Perry, 1995 #18055; Ripley, 1976). The fundamental question that we aim to

address is: given the locations of osteoblasts, are tumor cells found nearer to osteoblasts more often than would be expected by chance?

2D Analyses: In each section containing a tumor cell, the distance between the tumor cell and each senescent osteoblast in the image was computed and tabulated as an empirical distribution function. Formally, this function is defined follows:

$$\mathrm{EDF}(h) = \sum_{i}^{N} C_i(d \leq h) \qquad (2)$$

where h is distance, N is the number of senescent osteoblasts, and C_i is an indicator vector that takes a value of 1 if the distance between the tumor cell and j^{th} osteoblast is less than or equal to h and 0 otherwise. To determine whether this distribution of distances was likely by chance, we performed a Monte Carlo sampling with 10,000 replicates for each tumor cell testing against the null hypothesis commonly referred to as complete spatial randomness. In each sample, the senescent osteoblasts were assigned new random locations uniformly drawn from the entire region of interest, and the distance distribution to the tumor cell was recorded. Osteoblast locations were sampled instead of tumor cell locations to minimize edge effects associated with tumor cells located near the border of the region of interest. Following the sampling, the mean, standard deviation, median, and 95% confidence interval were computed. To allow for combination of data across multiple samples and mice, a normalized difference curve was computed.

The difference between the observed distance and mean difference for the n^{th} nearest osteoblast was taken and normalized by the sampling standard deviation. The resulting curve provides a measure of how many standard deviations away from the random mean the observed results lie. Thus, a normalized difference or effect size of 1 indicates that the average observed distance was closer than ~84% of the sampled distances. To allow us to present the data as a positive number when association was noted, we plotted the negative of the normalized difference (original graph is shown in **Figure S8**).

Cell culture. Primary osteoblasts were grown in culture medium (CM) containing ascorbic acid free alpha-MEM (Cat#A10490, Invitrogen, Grand Island, NY), 10% fetal bovine serum (FBS) (Cat#SH30109.03, Thermo Scientific, Logan, UT) and antibiotics (100U/ml of Penicillin and 100 ug/ml of Streptomycin, Cat#P0781, Sigma, Saint Louis, MO). To study the differentiation ability of senescent osteoblasts, cells were maintained in osteogenic medium (OM) consisting of alpha-MEM supplemented with 10% FBS, 50ug/ml ascorbic acid (Cat#A4544, Sigma, Saint Louis, MO) and 10mM β-glycerophosphate (Cat#G9422, Sigma, Saint Louis, MO). Bone marrow macrophages were cultured in alpha-MEM (Cat#12561, Invitrogen, Grand Island, NY) containing 10% FBS (Cat# 26140-079, Invitrogen, Grand Island, NY) and 10% CMG supernatant kindly provided by Dr. Deborah Novack, which was made as described previously (McHugh et al., 2000). 293T cells were cultured in DMEM with 10% FBS (Cat#F2442, Sigma, Saint Louis, MO) and antibiotics.

Primary Osteoblasts Isolation, Viral Transduction and Senescence Induction. Primary osteoblasts were isolated from the long bones as described previously (Bakker and Klein-Nulend, 2012). In brief, 6-week-old mice were sacrificed and long bones were removed, the ends of epiphyses were cut off and the bone marrow was removed by centrifugation. Following centrifugation bones were minced with a scissors till approximately 1-2mm^2 pieces were obtained. The bone pieces were washed with PBS and incubated in 4 ml collagenase II solution (2 mg collagenase II (Cat# 17101-015, Invitrogen, Grand Island, NY) per ml ascorbic acid free alpha-MEM) at 37°C incubator for 2 hours. The bone pieces were washed with CM and transferred to 10 cm dish. The medium was changed every 3 days.

Primary osteoblasts isolated from the FVB pure background FASST p27(+/+) and TRF2 mice were infected with pMSCVCre-ERpuro retrovirus. Virus was produced as previously described (Saharia and Stewart, 2009). Briefly, 293T cells were transfected with a mixture of the packaging plasmid pCLEco and retroviral DNA encoding the Cre-ER gene. To activate the p27 transgene, (or delete TRF2) stably transduced osteoblasts were treated with 10μM Tamoxifen (13258, Cayman Chemical Company, Ann Arbor, MI) or vehicle for 3 days and then stained for senescence-associated β-galactosidase activity. In brief, cells were fixed in 0.2% glutaraldehyde for 5 minutes at room temperature, washed with PBS, and stained with an X-gal solution (1mg/ml 5-Bromo-4-chloro-3-indolyl β-D-galactopyranoside (B4252, Sigma, Saint Louis, MO), 150mM NaCl, 2mM $MgCl_2$, 5mM $K_3Fe(CN)_6$ and 5 mM $K_4Fe(CN)_6$ in 40mM NaPi (PH 6.0) for 6-8 hours at 37°C. To induce

senescence with bleomycin, osteoblasts were treated with 6.7µl/ml bleomycin (B8416, Sigma, Saint Louis, MO) stocked at 15U/ml for 24 hours. Osteoblasts were consistently maintained at 3% O_2 at 37°C.

mRNA isolation and qRT-PCR. Total RNA was isolated from primary osteoblasts using the Ambion RiboPure RNA isolation kit (AM1924, Invitrogen, Grand Island, NY) according to the manufacturer's instructions. For cDNA synthesis, 1ug of RNA was reverse-transcribed using SuperScript II (18064-014, Invitrogen, Grand Island, NY) according to the manufacturer's instructions. The quantitative PCR was performed using a CFX96 Real-Time system (Bio-Rad, Hercules, CA) and Taqman gene expression assays for IL-6, ALP, RANKL, and OPG (4331182, Invitrogen, Grand Island, NY). GAPDH was used as the endogenous control (Taqman Assay 4352932E, Invitrogen, Grand Island, NY). To establish the impact of IL-6 neutralization on IL-6 expression, 10pg/µl of an IL-6 neutralization antibody (Cat#554400, BD Biosciences, San Jose, CA 95131) or IgG control (Cat#40041B, BioLegend, San Diego, CA 92121) was added to the senescent osteoblasts for 4 days and SASP expression was analyzed by RT-PCR.

Osteoblast Differentiation Assays. To assess differentiation, $1x10^5$ osteoblasts/well were plated onto 6 well plates in culture medium (CM). The following day medium was replaced with osteogenic medium, which was refreshed every 3 days. RNA isolation and Alkaline phosphatase staining was carried out on day 7 and Alizarin Red S staining was carried out on day 21.

Alkaline phosphatase staining was performed as previously described (Katagiri et al., 1994). In brief, osteoblasts were washed with PBS and fixed with 4% paraformaldehyde (PFA) for 10 minutes at room temperature. After washing with PBS, osteoblasts were incubated for 20 minutes with a mixture of 0.1 mg/ml Naphthol AS-MX phosphate (N4875, Sigma, Saint Louis, MO), 0.5% N,N-dimethylformamide (D4551, Sigma, Saint Louis, MO), 2mM MgCl2 and 0.6mg/ml fast blue BB Salt (F3378, Sigma, Saint Louis, MO) in 0.1M Tris/HCl, pH8.5, at room temperature.

For Alizarin Red-S staining, osteoblasts were fixed in 70% ethanol for 1 hour, rinsed with water and stained with 0.4% Alizarin Red-S (A5533, Sigma, Saint Louis, MO) (pH 4.1~4.3) for 10 minutes at room temperature, followed by an additional water wash.

Bone marrow macrophage (BMM) isolation and osteoblast-BMM co-culture assay. The long bones were removed from 6-week-old mice, the ends of the epiphyses were cut off and the BMM were removed by centrifugation and plated onto petri dishes in the medium as described above for 3-7 days. For the co-culture assay, $2x10^4$ senescent versus control osteoblasts and $1x10^5$ BMMs/well were plated into 24 well plates. 10 nM $1,25(OH)_2$ $VitD_3$ (D1530, Sigma, Saint Louis, MO) and 100 nM dexamethasone (D4902, Sigma, Saint Louis, MO) were added to the medium, which was replaced every other day. The cells were co-cultured for 4

days and then stained for tartrate-resistant acid phosphatase activity using the Acid Phosphatase, Leukocyte (TRAP) kit (387A, Sigma, Saint Louis, MO) according to the manufacturer's instructions. In brief, cells were incubated in fixative solution for 30 seconds and washed with PBS. Cells were stained by mixing 50µl Fast Garnet GBC base solution and 50µl Na-nitrite solution with 4.5ml water, 50ul Naphtol AS-BI-solution, 200µl Acetate solution and 100µl Tartrate solution together. The cells were stained with 400µl/well mixture in the dark at 37°C for 30 minutes. For IL-6 neutralization in this assay, senescent or non-senescent osteoblasts were co-cultured with BMMs and 5pg/µl of IL-6 neutralization antibody (Cat#554400, BD Biosciences, San Jose, CA 95131) or 5pg/µl of IgG control (Cat#40041B, BioLegend, San Diego, CA 92121) was added to the medium. The antibody was replenished every other day and mature osteoclasts formation was detected by TRAP staining on Day 4.

Osteoclast precursor proliferation assay. BMMs were co-cultured with either senescent or nonsenescent osteoblasts and the MTT assay was performed to measure BMMs proliferation at different time points (day 0, day 1 and day 3) per the manufacturers instructions. Briefly, 100µl 5mg/ml MTT was added to each well for 4hrs, the medium was removed, 1ml DMSO was added to each well, and the absorbance was read at 570nm.

Statistical analyses. All statistical analyses were carried out using Graftpad Prism. Numerical data are expressed as mean +/- SEM. Mouse analyses were performed

by Student's t test or Mann-Whitney test as indicated in the figure legends. Description of statistical analyses used in bone analysis of osteoclastogenesis and tumor localization can be found in the description of the computational approach in the methods section.

SUPPLEMENTAL REFERENCES

Bakker, A.D., and Klein-Nulend, J. (2012). Osteoblast isolation from murine calvaria and long bones. Methods in molecular biology (Clifton, NJ *816*, 19-29.

Filgueira, L. (2004). Fluorescence-based staining for tartrate-resistant acidic phosphatase (TRAP) in osteoclasts combined with other fluorescent dyes and protocols. J Histochem Cytochem *52*, 411-414.

Katagiri, T., Yamaguchi, A., Komaki, M., Abe, E., Takahashi, N., Ikeda, T., Rosen, V., Wozney, J.M., Fujisawa-Sehara, A., and Suda, T. (1994). Bone morphogenetic protein-2 converts the differentiation pathway of C2C12 myoblasts into the osteoblast lineage. J Cell Biol *127*, 1755-1766.

Lavine, K.J., Schmid, G.J., Smith, C.S., and Ornitz, D.M. (2008). Novel tool to suppress cell proliferation in vivo demonstrates that myocardial and coronary vascular growth represent distinct developmental programs. Dev Dyn *237*, 713-724.

McHugh, K.P., Hodivala-Dilke, K., Zheng, M.H., Namba, N., Lam, J., Novack, D., Feng, X., Ross, F.P., Hynes, R.O., and Teitelbaum, S.L. (2000). Mice lacking b3 integrins are osteosclerotic because of dysfunctional osteoclasts. Journal of Clinical Investigation *105*, 433-440.

Park, D., Spencer, J.A., Koh, B.I., Kobayashi, T., Fujisaki, J., Clemens, T.L., Lin, C.P., Kronenberg, H.M., and Scadden, D.T. (2012). Endogenous bone marrow

MSCs are dynamic, fate-restricted participants in bone maintenance and regeneration. Cell stem cell *10*, 259-272.

Perry, J.N. (1995). Spatial Analysis by Distance Indices. The Journal of Animal Ecology 64 *64*, 303.

Ripley, B.D. (1976). The Second-Order Analysis of Stationary Point Processes. Journal of Applied Probability *13*.

Saharia, A., and Stewart, S.A. (2009). FEN1 contributes to telomere stability in ALT-positive tumor cells. Oncogene *28*, 1162-1167.

Tsuboi, H., Matsui, Y., Hayashida, K., Yamane, S., Maeda-Tanimura, M., Nampei, A., Hashimoto, J., Suzuki, R., Yoshikawa, H., and Ochi, T. (2003). Tartrate resistant acid phosphatase (TRAP) positive cells in rheumatoid synovium may induce the destruction of articular cartilage. Annals of the rheumatic diseases *62*, 196-203.

Zheng, B., Zhang, Z., Black, C.M., de Crombrugghe, B., and Denton, C.P. (2002). Ligand-dependent genetic recombination in fibroblasts : a potentially powerful technique for investigating gene function in fibrosis. Am J Pathol *160*, 1609-1617.